



Universiteit
Leiden
The Netherlands

Correlations of spin splitting and orbital fluctuations due to $1/f$ charge noise in the Si/SiGe quantum dot

Kepa, M.; Cywinski, L.; Krzywda J.A.

Citation

Kepa, M., & Cywinski, L. (2023). Correlations of spin splitting and orbital fluctuations due to $1/f$ charge noise in the Si/SiGe quantum dot. *Applied Physics Letters*, 123(3).
doi:10.1063/5.0156358

Version: Publisher's Version

License: [Licensed under Article 25fa Copyright Act/Law \(Amendment Taverne\)](#)

Downloaded from: <https://hdl.handle.net/1887/3718681>

Note: To cite this publication please use the final published version (if applicable).

RESEARCH ARTICLE | JULY 18 2023

Correlations of spin splitting and orbital fluctuations due to 1/f charge noise in the Si/SiGe quantum dot

Special Collection: [Electronic Noise: From Advanced Materials to Quantum Technologies](#)

M. Kępa  ; Ł. Cywiński  ; J. A. Krzywda  

 Check for updates

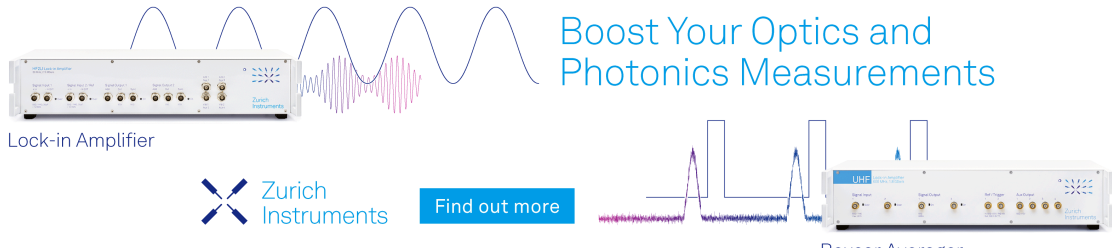
Appl. Phys. Lett. 123, 034003 (2023)

<https://doi.org/10.1063/5.0156358>




CrossMark

Boost Your Optics and Photonics Measurements



Lock-in Amplifier

 Zurich Instruments

[Find out more](#)

Boxcar Averager

Correlations of spin splitting and orbital fluctuations due to $1/f$ charge noise in the Si/SiGe quantum dot

Cite as: Appl. Phys. Lett. **123**, 034003 (2023); doi: [10.1063/5.0156358](https://doi.org/10.1063/5.0156358)

Submitted: 28 April 2023 · Accepted: 2 July 2023 ·

Published Online: 18 July 2023



View Online



Export Citation



CrossMark

M. Kępa,¹  Ł. Cywiński,¹  and J. A. Krzywda^{1,2,a)} 

AFFILIATIONS

¹Institute of Physics, Polish Academy of Sciences, al. Lotników 32/46, Warsaw PL 02-668, Poland

²Lorentz Institute and Leiden Institute of Advanced Computer Science, Leiden University, P.O. Box 9506, Leiden 2300 RA, The Netherlands

Note: This paper is part of the APL Special Collection on Electronic Noise: From Advanced Materials to Quantum Technologies.

^{a)}Author to whom correspondence should be addressed: krzywda@ifpan.edu.pl

ABSTRACT

Fluctuations in electric fields can change the position of a gate-defined quantum dot (QD) in a semiconductor heterostructure. In the presence of magnetic field gradient, these stochastic shifts of electron's wavefunction lead to fluctuations of electron's spin splitting. The resulting spin dephasing due to charge noise limits the coherence times of spin qubits in isotopically purified Si/SiGe quantum dots. We investigate the spin splitting noise caused by such a process due to microscopic motion of charges at the semiconductor-oxide interface. We compare effects of isotropic and planar displacement of the charges and estimate their densities and typical displacement magnitudes that can reproduce experimentally observed spin splitting noise spectra. We predict that for a defect density of 10^{10} cm^{-2} , visible correlations between noises in spin splitting and in energy of electron's ground state in the quantum dot are expected.

Published under an exclusive license by AIP Publishing. <https://doi.org/10.1063/5.0156358>

Due to the weakness of spin-orbit coupling in a conduction band of silicon and possibility of isotopic enrichment leading to removal of spinful ^{29}Si nuclei, a spin of a single electron in an isotopically purified silicon quantum dot (QD) has the longest coherence time of all the QD-based spin qubits.^{1–6} However, this relative isolation of the spin degree of freedom from external influences makes it hard to perform spin rotations, i.e., single-qubit quantum gates. The currently commonly accepted solution is to expose such qubits to magnetic field gradients generated by nearby nanomagnets.^{7–9} The gradients of magnetic fields transverse to a global quantization axis, due to constant external B field, allow then for dot-selective electron spin resonance operations driven by ac voltages on gates defining the QDs.^{2,10–13} The gradients of the longitudinal components of the magnetic field lead to qubit-specific spin splittings, further diminishing the addressing errors, when one of the two nearby qubits is driven by ac voltages with appropriately chosen frequency.^{14,15} However, the presence of the latter gradient makes the splitting of a given spin sensitive to fluctuations of electric fields, as charge-noise-induced fluctuations of an electron position translate into noise in its spin splitting.

Charge noise affecting electron's orbital energy levels has been recently characterized for many silicon-based QDs in heterostructures that are considered as platforms for a large-scale semiconductor-based quantum computer.^{13,16–19} This spurred theoretical investigations of microscopic models of $1/f$ charge noise that could reproduce the observed levels of electron orbital energy fluctuations in SiMOS²⁰ and Si/SiGe QDs.²¹ It is commonly assumed that the charge noise in such metal-insulator-semiconductor structures is due to dynamics of charged defects located at the semiconductor/oxide interface.^{20,22,23} Calculations in Refs. 20 and 21 have established that in order to reproduce the typical order of magnitude of $1/f$ charge noise seen in relevant QDs, the charges should remain trapped at the interface, switching between positions separated by $\delta r < 1 \text{ nm}$, i.e., acting as two-level fluctuators (TLFs). Ranges of densities, ρ of such TLFs, and values of δr that lead to reproduction of observed noise, were described in these papers. Here, we follow up on the study from Ref. 21 by adding a magnetic field gradient and considering fluctuations of spin splitting due to dynamics of sources of charge noise. A comparison of the results of the simulations with measured data on spin dephasing in Si/SiGe QDs exposed to B field gradient leads to further

narrowing down of ranges of parameters of the microscopic models of charge noise that are consistent with state-of-the-art experiments.

We use the model of the Si/SiGe QD device from Ref. 21 and start with the model of TLFs described there. Thus, we assume a typical, constant temperature of $T \approx 100$ mK and equal occupation of TLF states. We consider charges localized at random positions near the semiconductor-oxide interface, with ρ being their interface-averaged planar density, and assume that each of them switches between two positions, \mathbf{r}_n and $\mathbf{r}_n + \delta\mathbf{r}_n$, where the components of $\delta\mathbf{r}_n$ are drawn from independent Gaussian distributions of zero average and equal variances, such that $\langle |\mathbf{r}_n| \rangle = \langle \sqrt{\delta x^2 + \delta y^2 + \delta z^2} \rangle \equiv \delta r$ is the rms of charge displacement.

The model of the device consists of 600×600 nm² Si_{0.7}Ge_{0.3}-Si quantum well (QW), where electrons are trapped and located about 80 nm below the metallic electrodes, and has been implemented in COMSOL (see Ref. 21 for device description). Dashed overlay in Fig. 1(a) shows the outline of metallic gates and the channel. We compute the ground and first excited state of the stationary Schrodinger equation in a 10 nm high Si layer of QW using a built-in COMSOL eigenvalue solver. In this study, the voltage on the plunger gate in the middle of the device is set to 0.25 V, while keeping other gates grounded, giving a realistic orbital gap $\hbar\omega = E_1 - E_0 \approx 2$ meV. To

study the effect of charged defects, we define a 31×31 regular grid in the XY plane. At each point of the grid, and at four different heights $z_0 = 101.75, 102.0, 102.25, 102.5$ nm, close to the semiconductor-oxide interface, we place a single charge with $q = -|e|$. For each defect position, we extract the expectation values of position operator $\mathbf{R} \equiv \langle \psi | \hat{\mathbf{r}} | \psi \rangle = \int_V \mathbf{r} |\psi|^2 dV$, where ψ is the wavefunction of the ground state and V represents the volume of the Si layer. This procedure is followed by the interpolation.

In the presence of longitudinal magnetic field gradient, the displacement of the electron wavefunction is translated to a change in Zeeman splitting,

$$\delta\Omega(\mathbf{r}_n) = g\mu_B \Delta\mathbf{B}_{\parallel} \cdot \delta\mathbf{R}(\mathbf{r}_n), \quad (1)$$

where we used electronic g-factor g , Bohr magneton μ_B , $\Delta\mathbf{B}_{\parallel}$ as gradient of the longitudinal component of the magnetic field at the location of the QD, and $\delta\mathbf{R}(\mathbf{r}_n) = [X(\mathbf{r}_n), Y(\mathbf{r}_n), Z(\mathbf{r}_n)]^T$ as the shift of the QD position due to the presence of the defect at \mathbf{r}_n . For simplicity, in this paper, we will assume that the longitudinal field gradient is along the x-axis only, $\Delta\mathbf{B}_{\parallel} = (\Delta B_{\parallel}, 0, 0)^T$, i.e., in the direction parallel to the channel and perpendicular to metallic gates (see Fig. 1). To calibrate our results against experimental results, we use here $\Delta B_{\parallel} = 0.2$ mT/nm from Refs. 2 and 18, which in Si is equivalent to the gradient in Zeeman splitting $\Delta\Omega/\Delta X \approx 0.025$ $\mu\text{eV}/\text{nm}$. Gradient along a single direction means that the shift in spin splitting is sensitive to the change in the x-component of QD position only, i.e., $\delta\Omega(\mathbf{r}_n) = g\mu_B \Delta B_{\parallel} \delta X(\mathbf{r}_n)$.

The raw data are obtained using a finite element method implemented in COMSOL software, as described above, and presented in Fig. 1(a) for a single plane $z_0 = 102$ nm. The resulting shift in Zeeman splitting, $\delta\Omega$, is about four orders of magnitude smaller than the shift in orbital energy, δE computed for the same device in Ref. 21. In contrast to those results, we observe both increase and decrease in Ω , which can be understood as a motion of quantum dots to the right (along the gradient) and to the left (against the gradient), respectively, see Fig. 1(b) for the cartoon of the energy shift.

As in Ref. 21, we employ now the $1/f$ noise model of many independent TLFs corresponding to charges jumping between \mathbf{r}_n and $\mathbf{r}_n + \delta\mathbf{r}_n$, each being a source random telegraph noise characterized by switching rate γ_n sampled from a log-normal distribution.^{24–26} We consider switching rates $f_{\min} < \gamma_n < f_{\max}$, with experimentally relevant frequencies $f_{\min} = 10^{-6}$ Hz and $f_{\max} = 10^6$ Hz. We define the coupling between the TLF and the single electron spin qubit as

$$\zeta_n = \delta\Omega(\mathbf{r}_n + \delta\mathbf{r}_n) - \delta\Omega(\mathbf{r}_n) \approx \nabla\delta\Omega(\mathbf{r}_n) \cdot \delta\mathbf{r}_n. \quad (2)$$

We assume the contribution from multiple defects is additive, i.e., $\delta\Omega(\{\sum_n \mathbf{r}_n\}) = \sum_n \delta\Omega(\mathbf{r}_n)$. We have tested this assumption against the case of two charges located at random positions, which produced relatively small error $\delta\Omega(\mathbf{r}_1, \mathbf{r}_2) - \delta\Omega(\mathbf{r}_1) - \delta\Omega(\mathbf{r}_2) \ll 0.1$ neV. This allows us to compute the power spectral density (PSD) of the noise in Zeeman splitting for various charge densities ρ , and individual TLFs parameters: displacement size δr_n and switching rates γ_m without further finite-element simulations. Since each TLF is characterized by a Lorentzian spectrum, the total PSD reads

$$S_{\text{spin}}(f) = \sum_{n=1}^N \frac{2\zeta_n^2}{\gamma_n + (2\pi f)^2/\gamma_n}, \quad (3)$$

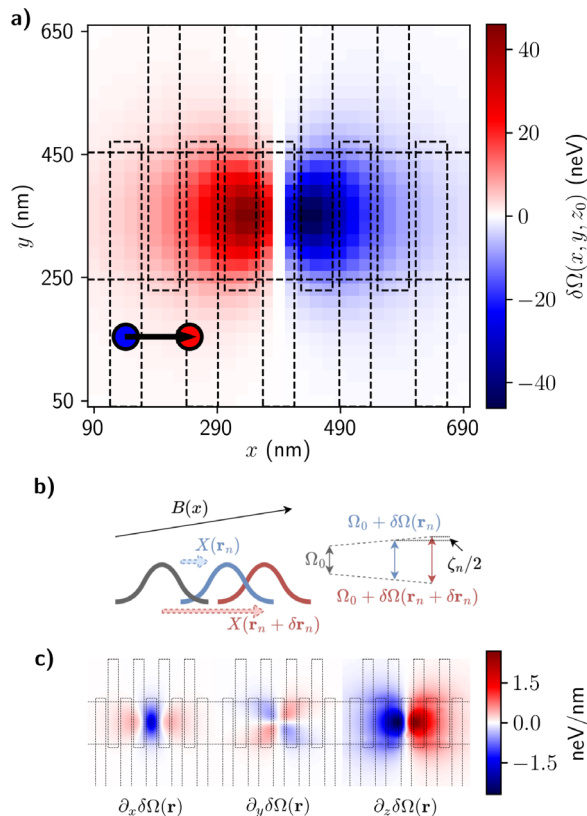


FIG. 1. (a) Modification of spin splitting $\delta\Omega(x, y, z_0)$ due to the presence of a charge defect located close to the semiconductor-oxide interface, i.e., at $\mathbf{r} = (x, y, z_0)$. (b) Illustration of $\delta\Omega$ caused by the shift of electron wavefunction $\Delta R(\mathbf{r})$ in the presence of magnetic field gradient $\Delta B_{\parallel} = 0.2$ mT/nm. (c) Derivatives along x, y, and z directions used later to compute the TLF-spin coupling $\zeta_n = \nabla\delta\Omega \cdot \delta\mathbf{r}_n$.

where the n -th TLF is characterized by coupling ζ_n and switching rate γ_n . For each realization, we first use the uniform spatial distribution to draw positions of N charges at $z_0 = 102$ nm plane, where $N = A\rho$ is related to charge density ρ and considered area A . Next, in each realization and for each charge, we draw the components of displacement vector $\delta\mathbf{r}_n$ from the independent Gaussian distribution of zero average and the equal variances such that $\langle |\mathbf{r}_n| \rangle = \langle \sqrt{\delta x^2 + \delta y^2 + \delta z^2} \rangle \equiv \delta r$ is the displacement size.

Using interpolated data from Fig. 1(a), we compute the gradients of spin splitting shifts in Fig. 1(c). In all directions, we observe that depending on the initial location, the motion of the defect can both increase and decrease Ω . By comparing the relative value of the gradient components, we see the same displacement of a charge along the z -direction results in noise larger by about an order of magnitude in comparison to the in-plane displacements. It is caused by the decrease in the distance between the charge and its image that is located in the metal. This effectively decreases the dipole moment of the charge-image pair. It can also be seen from similarity (with negative sign) between $\delta\Omega$ and $\partial_z\delta\Omega$. In the planar direction, the x -derivative is about two times larger than y -, which shows that the motion of the charge along the x direction is more effective at moving the electron's wavefunction along this direction (which is the direction of the gradient of the longitudinal field).

We now translate motion of multiple TLFs into spin splitting noise. We concentrate on slow fluctuations of spin splitting that directly affect the measured coherence time of spin qubit, $T_2^* = \sqrt{2}/\sigma_{\text{spin}}$, that is parameterized by the noise amplitude

$$\sigma_{\text{spin}}^2 = 2 \int_{f_{\min}}^{f_{\max}} S_{\text{spin}}(f) df \equiv \sum_n \zeta_n^2. \quad (4)$$

Since typically T_2^* varies between different QDs in isotopically purified Si/SiGe, as a reference we use both the longest-observed coherence time of $T_2^* \approx 20 \mu\text{s}$ from Refs. 2 and 13 and the much shorter $T_2^* = 1 \mu\text{s}$ from Ref. 18. Assuming $\Delta B_{\parallel} = 0.2$ mT/nm, these values can be related to $\sigma_{\text{spin}} = 1$ neV (Ref. 18), 0.05 neV (Ref. 2), and $\sigma_{\text{spin}} = 0.1$ neV (Ref. 13), for which we have increased the noise amplitude to compensate for twice smaller gradient. In Fig. 2(a), we show the statistics of the noise amplitude obtained from 1000 realizations of the isotropic model, for three different charge densities ρ (colors) as a function of the displacement size δr (x -axis). We mark the values of σ_{spin} from references above using dashed lines. For none of the selected pairs of ρ and δr , it is possible to reconstruct all of these values. Additionally, $\sigma_{\text{spin}} \leq 0.1$ neV corresponding to two^{2,13} has been reached only for extreme parameters, i.e., the smallest $\delta r = 0.1$ nm, and $\rho = 5 \times 10^9$ nm⁻². For larger densities, not more than a single reference value has been reached, independently of δr .

For this reason, we consider now an alternative model of charge motion constrained only to the $z_0 = 102$ nm plane. We show the result for such a planar motion model in Fig. 2(b). In comparison to the isotropic motion, we observe a small increase in the data spread and, more importantly, a decrease in the average noise amplitude by a factor of about 2. Those changes make the $\sigma_{\text{spin}} \leq 0.1$ neV much easier to achieve for a range of parameters, i.e., $\rho \leq 10^{10}$ cm⁻² and $\delta r \leq 0.5$ nm. Simultaneously, some of those parameters allowed also for reaching the largest considered $\sigma_{\text{spin}} = 1$ neV. Thus, a planar

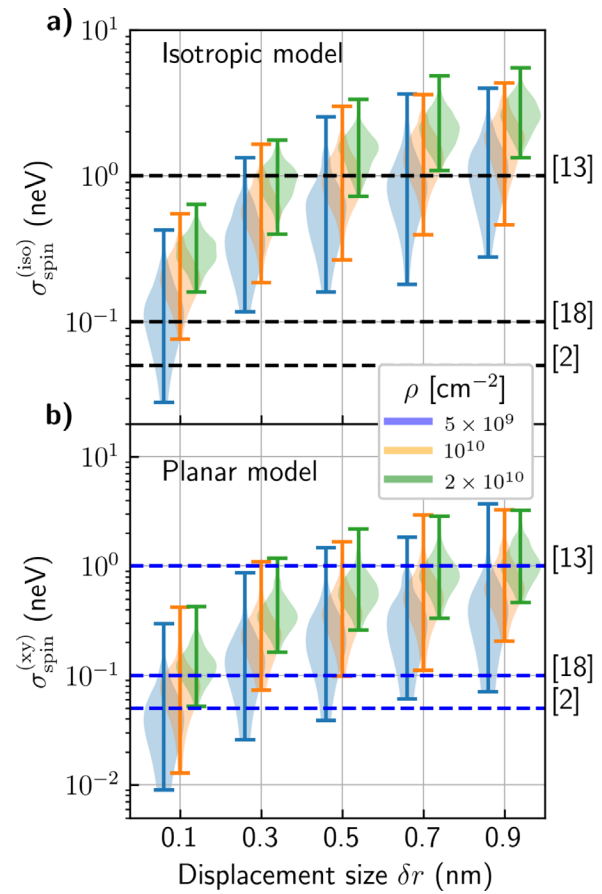


FIG. 2. Amplitude of spin splitting noise as a function of the typical displacement size for three different charge densities in the isotropic model (a) from Ref. 21 and the planar model. (b) Violins for given δr are slightly offset to increase the legibility of the figure. The numbers on the right correspond to noise amplitude from experimental Refs. 2, 13, and 18.

model performed better at reconstructing both ends of experimentally relevant values of σ_{spin} . We highlight that relatively larger variance of σ_{spin} , observed in the planar model, can be useful in distinguishing between the two models, given sufficiently large statistics of T_2^* across many experimental devices is collected.

In each model, both ensemble averages and standard deviations of σ_{spin} follow a linear trend with respect to δr with their proportionality factor having polynomial dependence on ρ (see Ref. 21 for analogous analysis, but for orbital noise). For the average σ_{spin} , we find effective expressions as

$$\begin{aligned} \langle \sigma_{\text{spin}}^{(xy)} \rangle &\approx \left[0.91 \left(\frac{\rho}{10^{10} \text{cm}^{-2}} \right)^{0.54} + 0.030 \right] \frac{\delta r}{\text{nm}} \text{ neV}, \\ \langle \sigma_{\text{spin}}^{(\text{iso})} \rangle &\approx \left[2.1 \left(\frac{\rho}{10^{10} \text{cm}^{-2}} \right)^{0.53} + 0.025 \right] \frac{\delta r}{\text{nm}} \text{ neV}. \end{aligned} \quad (5)$$

We use the fit from the above in Fig. 3(a), where we plot $\langle \sigma_{\text{spin}}^{(xy)} \rangle$ against δr and ρ .

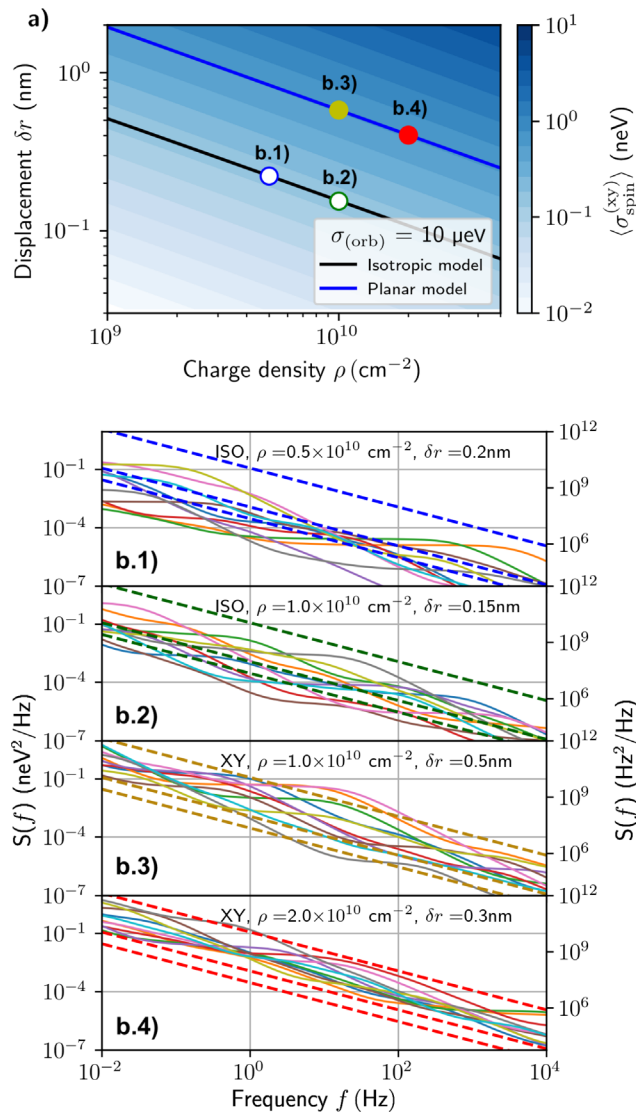


FIG. 3. (a) Fitted spin splitting noise amplitude $\langle \sigma_{\text{spin}}^{(xy)} \rangle$ in the XY model as a function of charge density ρ and displacement size δr . Using solid lines, we draw a cut through parameter space that corresponds to $\sigma_{\text{orb}} = 10 \mu\text{eV}$ of orbital energy fluctuations. Filled (hollow) dots correspond to a parameters used in panel (b) for planar (isotropic) models. (b) Ten realizations of power spectral densities of the spin splitting noise for four parameter pairs corresponding to colored dots in (a). For each dot, using the same color, we plot ideal 1/f spectra corresponding to $\sigma_{\text{spin}} = 0.05, 0.1, 1 \text{ neV}$ using dashed lines.

We also perform a cross-check and compute the amplitude of fluctuation of ground orbital level δE within the isotropic and planar model of charge motion. For the isotropic model, we use the final result of Ref. 21 and additionally compute the planar version using xy -gradients presented therein. In Fig. 3(a), we use the solid lines to plot the cut through parameter space that matches $\langle \sigma_{\text{orb}} \rangle = 10 \mu\text{eV}$, corresponding to $T_2^* \approx 0.1 \text{ ns}$ of the charge qubit,²⁷ that has been obtained in the isotropic (black) and planar (blue) models of charge motion. On

each of them, we chose two pairs of parameters $(\rho, \delta r)$. We mark then in Fig. 3(a) using colored dots, where hollow (filled) dots correspond to an isotropic (planar) model. For each of those points, in Fig. 3(b), we plot the corresponding PSD of the spin splitting noise and compare it with a PSD of ideal 1/f-shape,

$$S_{\text{spin}}(f) = \frac{\sigma_{\text{spin}}^2}{2 \ln(f_{\text{max}}/f_{\text{min}})} \times (1\text{Hz}/f), \quad (6)$$

calculated for reference values of $\sigma_{\text{spin}} = 0.05, 0.1, 1 \text{ neV}$.^{2,13,18}

In Fig. 3(b), we show exemplary ten realizations of random defect positions $\{\mathbf{r}_n\}$, their (isotropic/in-plane) displacement $\{\delta \mathbf{r}_n\}$, and switching rates $f_{\text{min}} < \{\gamma_n\} < f_{\text{max}}$. We report qualitative agreement between the obtained shapes and experimentally measured spectra,^{2,13,18} which can be seen from visible deviations from the 1/f trend due to distinct single TLF features (see also the discussion in Ref. 28). Those features are more prominent in the isotropic model, which can be seen to be the direct comparison of the PSDs obtained with $\rho = 10^{10} \text{ cm}^{-2}$ (two middle panels). On the other hand, such single TLF features are still present after an increase in ρ (last panel). Finally, we observe that quantitatively in the isotropic model, parameters $(\rho, \delta r)$ corresponding to $\sigma_{\text{orb}} = 10 \mu\text{eV}$ give smaller spin splitting than in the planar model. Also in the latter case, the resulting PSDs are a closer match to the dashed lines with the prominent example of $\rho = 10^{10} \text{ cm}^{-2}$ and $\delta r = 0.5 \text{ nm}$, and the realizations of which spread between all reference spectra (dashed lines).

We finally study the correlation between the orbital and spin splitting fluctuations. In analogy to Eqs. (3) and (4), we define the amplitude of low-frequency cross-correlated noise as

$$\sigma_{\Omega,E}^2 = \sum_n \zeta_n \eta_n, \quad (7)$$

where ζ_n (η_n) denotes coupling between the n -th TLF and the spin (ground orbital energy) of the electron. The contribution of each TLF to the correlated noise is then given by the product $\zeta_n \eta_n$. In Fig. 4(a), we show such a product for a single TLF located at $\mathbf{r}_n = (x, y, z_0)$ with displacement size $\delta r = 0.3 \text{ nm}$ along the x -axis (a), y -axis (b), and z -axis (c). We see that for the motion along these three primary directions, both positive and negative correlations of the noise processes are equally probable, which can be seen from the comparison between the sizes of red and blue regions. However, a non-negligible correlation requires the charge to be located in the central region around the QD.

We now analyze a relative correlation between orbital and spin splitting noise, defined via the normalized covariance

$$C_{\Omega,E} = \frac{\sigma_{\Omega,E}^2}{\sigma_{\Omega} \sigma_E}, \quad (8)$$

where $C_{\Omega,E} = \pm 1$ means perfectly correlated and anti-correlated noises, respectively, and $C_{\Omega,E} = 0$ means that the two fluctuations are uncorrelated. In Fig. 4(b), we plot $C_{\Omega,E}$ as a function of charge density ρ and for two displacement sizes, $\delta r = 0.1$ and 0.5 nm . From their comparison, we conclude that the correlation very weakly depends on δr . We also confirm that positively- and negatively correlated noises in Ω and E are equally probable (note the symmetry with respect to $C_{\Omega,E} = 0$). The noise is strongly correlated if the number of TLFs is low, with the extreme case of $N \approx 4$ for $\rho = 10^9 \text{ cm}^{-2}$, and becomes

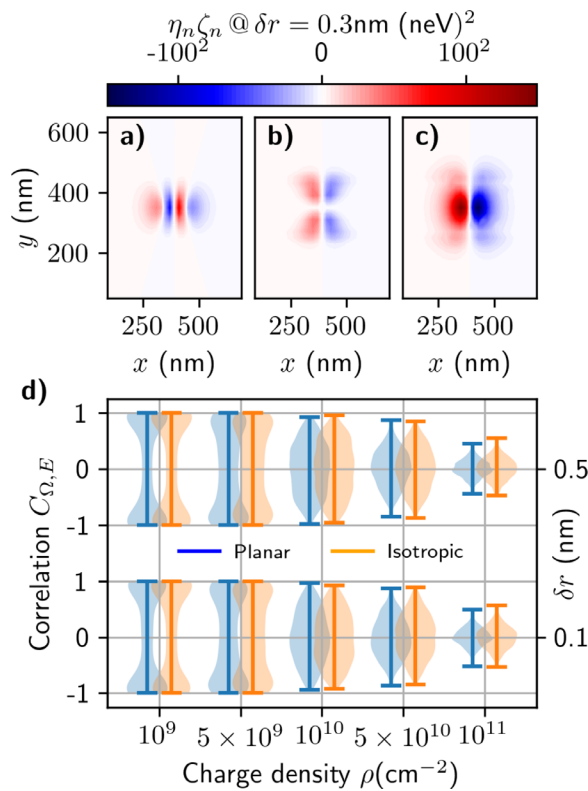


FIG. 4. Product of the couplings between a single defect at location $(x, y, z_0 = 102 \text{ nm})$ and spin (ζ_n) and orbital level (η_n) for defect displacement size of $\delta r = 0.3 \text{ nm}$ along x (a), y (b), and z (c) axes. (d) Correlation coefficient $C_{\Omega, E}$ between the fluctuations of ground orbital level E and spin splitting Ω as a function of defect density ρ and for two different displacement sizes $\delta r = 0.1, 0.5 \text{ nm}$. For low-densities, two quantities are correlated, and the correlation decreases with the increase in ρ .

weakly correlated if the number of TLFs is large, with $N=400$ at $\rho = 10^{11} \text{ cm}^{-2}$ as an example. In the former case, this is because the noise is typically dominated by a few or even a single TLF located in the central region of Fig. 4(a), for which the correlations are large. As ρ increases, both red and blue regions of Fig. 4(a) become equally populated, and also contributions from the regions in which the cross-correlations are weak increase. We report that correlations obtained in the isotropic and planar model of charge motion are similar. We also highlight that at the expected densities of $\rho = 10^{10} \text{ cm}^{-2}$, a relatively wide distribution of $C_{\Omega, E}$ is predicted, which means that a correlation between $\delta\Omega$ and δE is expected to vary visibly between similar devices or spatially distant regions of the same device.

In summary, building upon the model of the device and $1/f$ charge noise previously introduced in Ref. 21, we have simulated the influence of charge noise on the spin splitting of an electron in a single quantum dot in a Si/SiGe device, in the presence of magnetic field gradient of the magnitude used in spin qubit manipulation experiments. While in previous modeling,²¹ isotropic motion of TLF charges was assumed, here we have introduced a planar model, in which defects were allowed to move only in the plane parallel to the interface. We

have found that the planar motion of defects allowed for better agreement with experimentally measured spin splitting noise. We have predicted values of density of TLFs, $\rho \approx 10^{10} \text{ cm}^{-2}$ and the typical magnitude of motion of charges associated with them, $\delta r \approx 0.5 \text{ nm}$, that give results that are consistent with measured orbital energy fluctuations, as well as with other theoretical works.^{19,20,29} For this density, noise in spin splitting and in orbital energy should exhibit visible correlations. We believe further distinction between the planar and isotropic model can be made if also spatial correlations of orbital and spin-splitting noise are computed.

This research was funded in whole by the National Science Centre, Poland, Grant No. 2021/41/N/ST3/02758.

AUTHOR DECLARATIONS

Conflict of Interest

The authors have no conflicts to disclose.

Author Contributions

Marcin Kępa: Investigation (equal); Software (lead); Validation (lead); Visualization (lead). **Lukasz Cywinski:** Conceptualization (equal); Formal analysis (equal); Project administration (equal); Supervision (equal); Writing – original draft (equal); Writing – review & editing (equal). **Jan Adrian Krzywda:** Conceptualization (equal); Formal analysis (equal); Investigation (equal); Methodology (equal); Project administration (equal); Supervision (equal); Writing – original draft (equal); Writing – review & editing (equal).

DATA AVAILABILITY

The data that support the findings of this study are available from the corresponding author upon reasonable request.

REFERENCES

- ¹K. W. Chan, W. Huang, C. H. Yang, J. C. Hwang, B. Hensen, T. Tanttu, F. E. Hudson, K. M. Itoh, A. Laucht, A. Morello, and A. S. Dzurak, "Assessment of a silicon quantum dot spin qubit environment via noise spectroscopy," *Phys. Rev. Appl.* **10**, 1 (2018).
- ²J. Yoneda, K. Takeda, T. Otsuka, T. Nakajima, M. R. Delbecq, G. Allison, T. Honda, T. Kodera, S. Oda, Y. Hoshi, N. Usami, K. M. Itoh, and S. Tarucha, "A quantum-dot spin qubit with coherence limited by charge noise and fidelity higher than 99.9%," *Nat. Nanotechnol.* **13**, 102 (2018).
- ³T. Tanttu, B. Hensen, K. W. Chan, C. H. Yang, W. W. Huang, M. Fogarty, F. Hudson, K. Itoh, D. Culcer, A. Laucht, A. Morello, and A. Dzurak, "Controlling spin-orbit interactions in silicon quantum dots using magnetic field direction," *Phys. Rev. X* **9**, 021028 (2019).
- ⁴D. M. Zajac, A. J. Sigillito, M. Russ, F. Borjans, J. M. Taylor, G. Burkard, and J. R. Petta, "Resonantly driven CNOT gate for electron spins," *Science* **359**, 439–442 (2018).
- ⁵A. R. Mills, C. R. Guinn, M. J. Gullans, A. J. Sigillito, M. M. Feldman, E. Nielsen, and J. R. Petta, "Two-qubit silicon quantum processor with operation fidelity exceeding 99%," *Sci. Adv.* **8**, eabn5130 (2022).
- ⁶S. G. J. Philips, M. T. Madzik, S. V. Amitonov, S. L. de Snoo, M. Russ, N. Kalhor, C. Volk, W. I. L. Lawrie, D. Brousse, L. Tryputen, B. P. Wuetz, A. Sammak, M. Veldhorst, G. Scappucci, and L. M. K. Vandersypen, "Universal control of a six-qubit quantum processor in silicon," *Nature* **609**, 919–924 (2022).
- ⁷Y. Tokura, W. G. van der Wiel, T. Obata, and S. Tarucha, "Coherent single electron spin control in a slanting Zeeman field," *Phys. Rev. Lett.* **96**, 047202 (2006).

- ⁸R. Neumann and L. R. Schreiber, "Coherent single electron spin control in a slanting Zeeman field," *J. Appl. Phys.* **117**, 193903 (2015).
- ⁹M. Aldeghi, R. Allenspach, and G. Salis, "Modular nanomagnet design for spin qubits confined in a linear chain," *Appl. Phys. Lett.* **122**, 134003 (2023).
- ¹⁰K. Takeda, J. Kamioka, T. Otsuka, J. Yoneda, T. Nakajima, M. R. Delbecq, S. Amaha, G. Allison, T. Kodera, S. Oda, and S. Tarucha, "A fault-tolerant addressable spin qubit in a natural silicon quantum dot," *Sci. Adv.* **2**, e1600694 (2016).
- ¹¹R. Zhao, T. Tantt, K. Y. Tan, B. Hensen, K. W. Chan, J. C. C. Hwang, R. C. C. Leon, C. H. Yang, W. Gilbert, F. E. Hudson, K. M. Itoh, A. A. Kiselev, T. D. Ladd, A. Morello, A. Laucht, and A. S. Dzurak, "Single-spin qubits in isotopically enriched silicon at low magnetic field," *Nat. Commun.* **10**, 5500 (2019).
- ¹²A. Corna, L. Bourdet, R. Maurand, A. Crippa, D. Kotekar-Patil, H. Bohuslavskyi, R. Laviéville, L. Hutin, S. Barraud, X. Jehl, M. Vinet, S. De Franceschi, Y.-M. Niquet, and M. Sanquer, "Electrically driven electron spin resonance mediated by spin-valley-orbit coupling in a silicon quantum dot," *NPJ Quantum Inf.* **4**, 6 (2018).
- ¹³T. Struck, A. Hollmann, F. Schauer, O. Fedorets, A. Schmidbauer, K. Sawano, H. Riemann, N. V. Abrosimov, Ł. Cywiński, D. Bougeard, and L. R. Schreiber, "Low-frequency spin qubit detuning noise in highly purified ²⁸Si/SiGe," *NPJ Quantum Inf.* **6**, 40 (2020).
- ¹⁴R. Li, L. Petit, D. P. Franke, J. P. Dehollain, J. Helsen, M. Steudtner, N. K. Thomas, Z. R. Yoscovits, K. J. Singh, S. Wehner, L. M. K. Vandersypen, J. S. Clarke, and M. Veldhorst, "A crossbar network for silicon quantum dot qubits," *Sci. Adv.* **4**, eaar3960 (2018).
- ¹⁵I. Heinz and G. Burkard, "Crosstalk analysis for single-qubit and two-qubit gates in spin qubit arrays," *Phys. Rev. B* **104**, 045420 (2021).
- ¹⁶E. J. Connors, J. Nelson, H. Qiao, L. F. Edge, and J. M. Nichol, "Low-frequency charge noise in Si/SiGe quantum dots," *Phys. Rev. B* **100**, 165305 (2019).
- ¹⁷E. J. Connors, J. Nelson, L. F. Edge, and J. M. Nichol, "Charge-noise spectroscopy of Si/SiGe quantum dots via dynamically-decoupled exchange oscillations," *Nat. Commun.* **13**, 940 (2022).
- ¹⁸J. Yoneda, J. S. Rojas-Arias, P. Stano, K. Takeda, A. Noiri, T. Nakajima, D. Loss, and S. Tarucha, "Noise-correlation spectrum for a pair of spin qubits in silicon," [arXiv:2208.14150](https://arxiv.org/abs/2208.14150) (2022).
- ¹⁹J. S. Rojas-Arias, A. Noiri, P. Stano, T. Nakajima, J. Yoneda, K. Takeda, T. Kobayashi, A. Sammak, G. Scappucci, D. Loss, and S. Tarucha, "Spatial noise correlations beyond nearest-neighbor in ²⁸Si/SiGe spin qubits," [arXiv:2302.11717](https://arxiv.org/abs/2302.11717) (2023).
- ²⁰M. M. E. K. Shehata, G. Simion, R. Li, F. A. Mohiyaddin, D. Wan, M. Mongillo, B. Govoreanu, I. Radu, K. De Greve, and P. Van Dorpe, "Modelling semiconductor spin qubits and their charge noise environment for quantum gate fidelity estimation," [arXiv:2210.04539](https://arxiv.org/abs/2210.04539) (2022).
- ²¹M. Kepp, N. Focke, Ł. Cywiński, and J. A. Krzywda, "Simulation of 1/f charge noise affecting a quantum dot in a Si/SiGe structure," [arXiv:2303.13968](https://arxiv.org/abs/2303.13968) (2023).
- ²²D. Culcer and N. M. Zimmerman, "Dephasing of Si singlet-triplet qubits due to charge and spin defects," *Appl. Phys. Lett.* **102**, 232108 (2013).
- ²³B. P. Wuetz, D. D. Esposti, A.-M. J. Zwerver, S. V. Amitonov, M. Botifoll, J. Arbiol, A. Sammak, L. M. K. Vandersypen, M. Russ, and G. Scappucci, "Reducing charge noise in quantum dots by using thin silicon quantum wells," *Nat. Commun.* **14**(1), 1385 (2023).
- ²⁴J. Schrieffl, Y. Makhlin, A. Shnirman, and G. Schön, "Decoherence from ensembles of two-level fluctuators," *New J. Phys.* **8**, 1 (2006).
- ²⁵X. You, A. A. Clerk, and J. Koch, "Positive- and negative-frequency noise from an ensemble of two-level fluctuators," *Phys. Rev. Res.* **3**, 013045 (2021).
- ²⁶A. Shnirman, G. Schön, I. Martin, and Y. Makhlin, "Low- and high-frequency noise from coherent two-level systems," *Phys. Rev. Lett.* **94**, 127002 (2005).
- ²⁷Z. Shi, C. B. Simmons, D. R. Ward, J. R. Prance, R. T. Mohr, T. S. Koh, J. K. Gamble, X. Wu, D. E. Savage, M. G. Lagally, M. Friesen, S. N. Coppersmith, and M. A. Eriksson, "Coherent quantum oscillations and echo measurements of a Si charge qubit," *Phys. Rev. B* **88**, 075416 (2013).
- ²⁸U. Gunggördü and J. P. Kestner, "Indications of a soft cutoff frequency in the charge noise of a Si/SiGe quantum dot spin qubit," *Phys. Rev. B* **99**, 081301 (2019).
- ²⁹B. Shalakh, C. Delerue, and Y.-M. Niquet, "Modelling of spin decoherence in a Si hole qubit perturbed by a single charge fluctuator," [arXiv:2210.10476](https://arxiv.org/abs/2210.10476) (2022).